

R. LISIECKI^{1,✉}
W. RYBA-ROMANOWSKI¹
T. ŁUKASIEWICZ²

Relaxation of excited states of Tm^{3+} and $\text{Tm}^{3+}-\text{Eu}^{3+}$ energy transfer in YVO_4 crystal

¹ Institute of Low Temperature and Structure Research, Polish Academy of Sciences, ul. Okólna 2, 50-950 Wrocław, Poland

² Institute of Electronic Materials Technology, Wolczynska 133, 01-919 Warsaw, Poland

Received: 20 October 2005/Revised version: 16 January 2006
Published online: 14 March 2006 • © Springer-Verlag 2006

ABSTRACT $\text{Tm}^{3+}-\text{Eu}^{3+}$ energy transfer processes and relaxation dynamics of the ${}^3\text{H}_4$ and ${}^3\text{F}_4$ excited states of Tm^{3+} ions in 1 at. % Tm^{3+} , 5 at. % $\text{Eu}^{3+}:\text{YVO}_4$ single crystal were studied. Contribution of $\text{Tm}^{3+}-\text{Eu}^{3+}$ energy transfer reduces effectively the lifetime of terminal level in a potential ${}^3\text{H}_4-{}^3\text{F}_4$ laser transition at around 1.48 μm . Adverse quenching of the ${}^3\text{H}_4$ emission by Eu^{3+} ions is found to be less efficient than that reported for $\text{Tm}^{3+} + \text{Tb}^{3+}$ system in YVO_4 . The classical Inokuti–Hirayama model accounts well for an experimental decay curve of the ${}^3\text{H}_4$ emission recorded for co-doped crystal. Stimulated emission cross section for ${}^3\text{H}_4-{}^3\text{F}_4$ transition of Tm^{3+} at around 1.48 μm was analyzed taking into account the anisotropy of YVO_4 crystal.

PACS 42.55.Xi; 42.62.Fi

1 Introduction

YVO_4 crystal doped with neodymium has been a well-known laser material for last forty years [1]. Laser operation in YVO_4 containing 5 at. % of Tm^{3+} for transition ${}^3\text{F}_4-{}^3\text{H}_6$ was demonstrated later [2]. $\text{YVO}_4:\text{Tm}$ system emitting near 1.8 μm is of interest as a source of light in the near infrared, considerably less dangerous for human eye than neodymium-doped materials. The laser performance of crystals and glasses doped with trivalent thulium was evaluated extensively [3]. An inconvenience of laser action associated with the ${}^3\text{F}_4-{}^3\text{H}_6$ transition of thulium is related to its quasi three level scheme involving re-absorption losses [3].

Structure of energy levels of Tm^{3+} offers also a possibility of obtaining potentially more efficient four-level laser operation associated with the ${}^3\text{H}_4-{}^3\text{F}_4$ transition near 1.45 μm . The spectroscopic and laser properties of thulium in this spectral range, which is advantageous for telecommunication purposes, were studied in the fluoride crystals LiYF_4 [4–6] and BaYb_2F_8 [7] as well as in the oxide material $\text{SrGdGa}_3\text{O}_7$ [8]. In all these crystalline materials, the lifetime of the ${}^3\text{F}_4$ terminal laser level is longer than that of the ${}^3\text{H}_4$ initial level what makes laser operation self-terminated. A forced simultaneous oscillation of the ${}^3\text{H}_4-{}^3\text{F}_4$ and ${}^3\text{F}_4-{}^3\text{H}_6$ transitions is

one of the methods that may overcome the shortcoming [9]. Another method used to overcome the problem may consist of additional doping with Tb^{3+} [4] or Eu^{3+} ions [6]. It was found that Tb^{3+} ions actually shorten the ${}^3\text{F}_4$ lifetime but they quench adversely the ${}^3\text{H}_4$ emission [8]. The potential generation channel that makes use of the ${}^3\text{H}_4-{}^3\text{F}_4$ transition near 1.45 μm in $\text{YVO}_4:\text{Tm}$, Tb has been examined by Ermeneux et al. [10].

In this paper we examine the co-doping of $\text{YVO}_4:\text{Tm}$ with europium ions because their level structure is less favourable for the depletion of the ${}^3\text{H}_4$ level by $\text{Tm}-\text{Eu}$ energy transfer.

2 Experimental details

Single crystal of YVO_4 grown by the Czochralski technique containing 1 at. % of Tm^{3+} and 5 at. % of Eu^{3+} has been investigated. The content of thulium and europium ions in the crystal was checked by inductively coupled plasma (ICP) method. Concentrations of Tm^{3+} and Eu^{3+} measured were 0.98 at. % and 4.77 at. % respectively. Absorption spectra were recorded with a Varian 5E UV-VIS-IR spectrophotometer. Polarised emission spectra in the near infrared were recorded using a set-up consisting of Dongwoo Optron DM 711 monochromator equipped with a photomultiplier or InGaAs detector and a PC computer. A krypton ion laser provided cw excitation in the red light range. To record luminescence decay curves in the infrared region (1100–2100 nm) a SPM 2 monochromator equipped with a cooled EG&G InSb detector was used. Luminescence decay curves in the visible and IR range were recorded with a Tektronix Model TDS 3052 digital oscilloscope following the short pulse excitation by Continuum Surelite I optical parametric oscillator (OPO) pumped by the third harmonic of a Nd:YAG laser.

3 Results and discussion

A survey absorption spectrum of Tm^{3+} and Eu^{3+} in YVO_4 recorded at room temperature with unpolarized light is shown in Fig. 1. The spectrum in the 3000–14000 cm^{-1} spectral region consists of three bands corresponding to transitions from the ground ${}^3\text{H}_6$ multiplet to the ${}^3\text{F}_4$, ${}^3\text{H}_5$ and ${}^3\text{H}_4$ multiplets of thulium and at longer wavelength from the ground multiplet ${}^7\text{F}_0$ to the ${}^7\text{F}_{4-6}$ levels of europium. Corresponding energy level scheme is shown in Fig. 2. For the purpose of optical pumping the band situated

✉ Fax: (48-71) 344 10 29, E-mail: Lisiecki@int.pan.wroc.pl

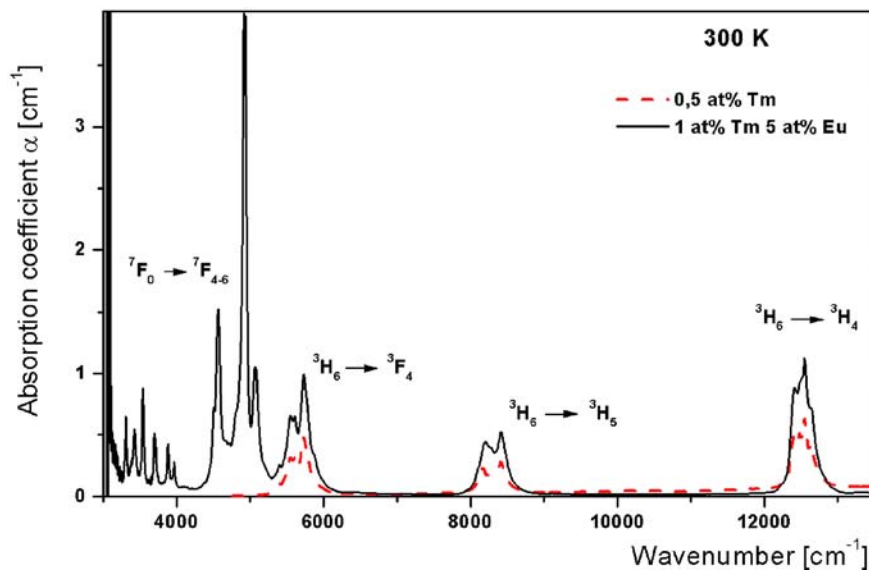


FIGURE 1 Unpolarized absorption spectrum for Tm^{3+} , Eu^{3+} in the YVO_4 at 300 K

between 12000 and 13000 cm^{-1} (750–850 nm) is relevant, since it perfectly matches the emission wavelength of commercial high-power AlGaAs laser diodes. The intensity of this broad and unresolved band is advantageously high. The maximum peak value of the absorption cross-section σ_{abs} was found to be $2.87 \times 10^{-20} \text{ cm}^2$ at 797.5 nm [11]. Incorporation of europium ions to selective transfer of energy from 3F_4 level of Tm^{3+} to the 7F_6 multiplet of Eu^{3+} is expected to provide a simple depopulation scheme for terminal 3F_4 level of thulium. It can be seen in Fig. 1 that the Eu^{3+} ions do not absorb at around 800 nm; thus, they will not reduce the pumping efficiency under laser diode excitation. It follows from Fig. 2 that there is an energy mismatch between 7F_6 level of Eu^{3+} and 3F_4 of Tm^{3+} and energy transfer from both the 3F_4 and 3H_4 emitting levels of Tm^{3+} in YVO_4 to acceptor Eu^{3+} ions is supposed to be phonon-assisted. The excited 7F_J multiplets of Eu^{3+} will decay very rapidly to the ground state via multiphonon relaxation thus Eu^{3+} – Tm^{3+} back transfer is hardly possible. Inspection of Tm^{3+} energy level scheme (see Fig. 2) leads to the conclusions that $\text{YVO}_4:\text{Tm}^{3+}$, Eu^{3+} system may be pumped into the 3H_4 level effectively because optical losses

such as ESA of pump radiation around 800 nm are not likely to occur.

To obtain the interaction parameters characterizing the energy-transfer processes single and co-doped samples were examined. The decay curves from 3F_4 level in 0.5 at. % $\text{Tm}^{3+}:\text{YVO}_4$, 6 at. % $\text{Tm}^{3+}:\text{YVO}_4$ and 1 at. % Tm^{3+} + 5 at. % $\text{Eu}^{3+}:\text{YVO}_4$ samples were measured for the 3F_4 – 3H_6 luminescence transitions at around 1.8 μm (see Fig. 3). In the crystal singly doped with thulium decay curves are clearly exponential for both 0.5 at. % Tm and 6 at. % Tm concentrations. However, concentration-dependent quenching process is evidenced by shortening of the 3F_4 lifetime from about 1.9 ms to 1.4 ms when Tm^{3+} concentration increases from 0.5 at. % to 6 at. %. The origin of this quenching is not clear. It might be caused by migration of accelerated energy transfer to traps of unknown nature. At a higher thulium concentration the 3H_4 excitation is transferred to the 3F_4 level by a cross relaxation process (see Fig. 2) and the laser operation associated with the 3F_4 – 3H_6 transition becomes feasible. In contrast to laser operation near 1800 nm the generation around 1480 nm associated with the 3H_4 – 3F_4 transition requires low doping level to reduce the cross-relaxation losses. The 3F_4 lumines-

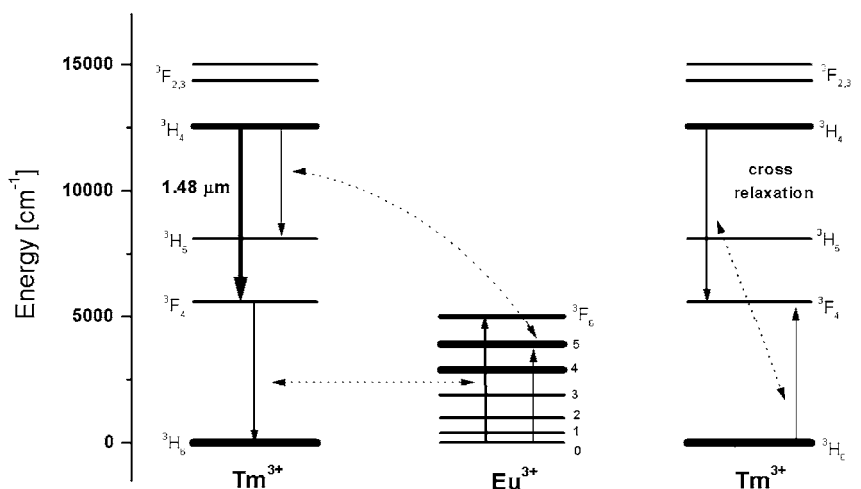


FIGURE 2 The energy level diagram of Tm^{3+} , Eu^{3+} ions in the YVO_4 crystal and energy transfer as well as cross-relaxation processes among activator ions

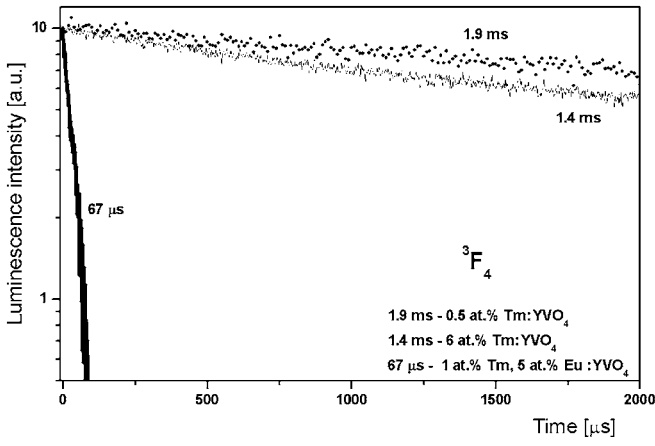
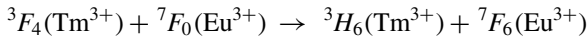


FIGURE 3 Decay curves of the 3F_4 luminescence for samples containing 0.5 at. % Tm^{3+} ; 6 at. % Tm^{3+} and 1 at. % Tm^{3+} , 5 at. % Eu^{3+} recorded at room temperature

cence lifetime of Tm^{3+} in a sample co-doped with Eu^{3+} ions is advantageously short and amounts to 67 μs . The direct energy transfer from 3F_4 level of Tm^{3+} to unexcited Eu^{3+} ions proceeds according to the scheme:



Efficiency η of energy transfer defined as $\eta = 1 - (\tau/\tau_0)$ where τ_0 is an intrinsic lifetime of donor is close to 0.95.

Using room temperature unpolarized absorption spectra corresponding to ${}^3H_6-{}^3F_4$ transition, we have calculated the stimulated emission cross sections $\sigma_{\text{em}}(\lambda)$ according to the formula:

$$\sigma_{\text{em}}(\lambda) = \frac{Z_{\text{low}}}{Z_{\text{up}}} \sigma_a(\lambda) \exp\left(\frac{Z_{\text{ZL}} - E(\lambda)}{k_B T}\right) \quad (1)$$

Where $\sigma_a(\lambda)$ is an absorption cross section and Z_{low} , Z_{up} are partition functions for lower and upper states respectively, defined as:

$$Z_{\text{low}} = \sum_{i=1}^n g_i \exp\left(\frac{-E_i}{k_B T}\right)$$

$$Z_{\text{up}} = \sum_{j=1}^n g_j \exp\left(\frac{-(E_j - E(\lambda))}{k_B T}\right) \quad (2)$$

where g_i (g_j) are the degeneracies of crystal field levels, E_i (E_j) are energies of crystal field levels, E_{ZL} is the energy separation between the lowest crystal field levels of upper and lower states, and k_B is the Boltzmann constant. For this calculation energies of the crystal field levels of the two multiplets were taken from [12]. Measured unpolarized absorption cross sections for transitions ${}^3H_6-{}^3F_4$ of Tm^{3+} and ${}^7F_0-{}^7F_6$ of Eu^{3+} as well as derived stimulated emission cross sections for transitions ${}^3F_4-{}^3H_6$ are shown in Fig. 4. The critical radius R_{DA} for energy transfer can be estimated from the overlap integral of the absorption and emission spectra of the donor and acceptor ions by using the formula [6]:

$$R_{\text{DA}}^6 = \frac{3c\tau_R}{8\pi^4 n^2} \int \sigma_{\text{em}}^D(\lambda) \sigma_{\text{abs}}^A(\lambda) d\lambda \quad (3)$$

where n is the refractive index of the material, τ_R is the radiative lifetime of the donor, σ_{em}^D is the stimulated emission cross section of the donor, and σ_{abs}^A is the absorption cross section of the acceptor. In the case of dipole-dipole transfer mechanism the energy transfer microparameters C_{DA} and the energy transfer probability P_{DA} are defined by [6]:

$$C_{\text{DA}} = \left(\frac{1}{\tau_R}\right) (R_{\text{DA}})^6 \quad P_{\text{DA}} = C_{\text{DA}} R_{\text{DA}}^{-6} \quad (4)$$

The critical radius R_{DA} for energy transfer from 3F_4 of Tm^{3+} in YVO_4 calculated using the integral σ_{em}^D (Tm^{3+}) and σ_{abs}^A (Eu^{3+}) derived from the spectra shown in Fig. 4 amounts to $R_{\text{DA}} = 5.95 \text{ \AA}$ and resulting microparameter $C_{\text{DA}} = 2.21 \times 10^{-41} \text{ cm}^6 \text{ s}^{-1}$. In this calculation the 3F_4 luminescence lifetime measured for a singly doped sample containing 0.5 at. % of Tm^{3+} was assumed to be equal to the 3F_4 radiative lifetime. The derived parameters are significantly smaller than the $R_{\text{DA}} = 14.84 \text{ \AA}$ and $C_{\text{DA}} = 7.58 \times 10^{-40} \text{ cm}^6 \text{ s}^{-1}$ reported for energy transfer from the 3F_4 in $\text{LiYF}_4:\text{Tm}^{3+}, \text{Eu}^{3+}$ [5]. This is due to the fact that the $\text{Tm}^{3+}-\text{Eu}^{3+}$ energy transfer is not resonant and is supposed phonon-assisted. In consequence the overlap integral derived from the absorption and emission spectra associated with electronic transitions is very small. In the calculation of overlap integral for the $\text{LiYF}_4:\text{Tm}^{3+}, \text{Eu}^{3+}$ system the contribution of phonon sidebands has been included by constructing the phonon sidebands for each transitions, according to exponential laws proposed by Auzel [13]. In our calculation the phonon sidebands were not considered; therefore, the derived overlap integral appears to be underestimated.

In contrast to the 3F_4 relaxation the decay curve of luminescence originating from the 3H_4 level in 1 at. % Tm^{3+} , 5 at. % $\text{Eu}^{3+}:\text{YVO}_4$ was non exponential (see Fig. 5). To receive information about non-radiative energy transfer processes the analysis of luminescence decay curves of donors may be performed using theoretical models proposed by Yokota-Tanimoto [14] and Inokuti-Hirayama [15]. The former model takes into account the excitation energy migration over donor system. The latter model applies when the donor concentration is sufficiently low to neglect the donor-donor interaction. According to Inokuti-Hirayama, the time depen-

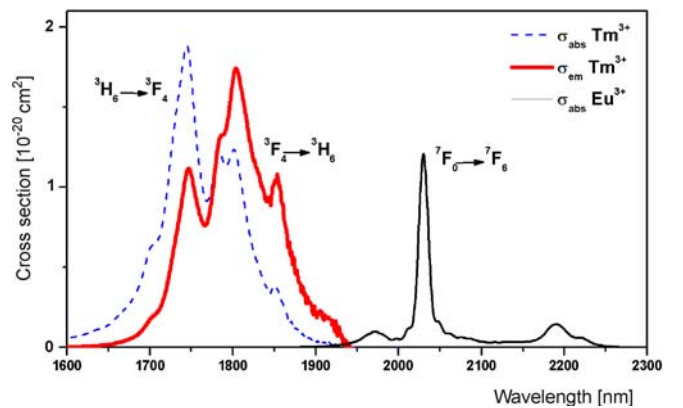


FIGURE 4 Emission cross section for transition ${}^3F_4-{}^3H_6$ of Tm^{3+} and absorption cross section for transitions ${}^3H_6-{}^3F_4$ of Tm^{3+} and ${}^7F_0-{}^7F_6$ of Eu^{3+} in YVO_4

dence of donor luminescence $\Phi(t)$ in the presence of acceptors is expressed by:

$$\Phi(t) = A \exp \left[-\frac{t}{\tau_0} - \alpha \left(\frac{t}{\tau_0} \right)^{\frac{3}{k}} \right] \quad (5)$$

where A is a constant, $\Phi(t)$ is emission intensity after pulse excitation, $k = 6$ for dipole–dipole interactions between ions, τ_0^{-1} is the intrinsic decay probability of donor ions involved in the energy transfer process in the absence of acceptors and α is the parameter described as:

$$\alpha = \frac{4}{3} \pi \Gamma (1 - 3/k) C_A R_{DA}^3 \quad (6)$$

In (6) $k = 6$, thus $\Gamma(1 - 3/k) = \Gamma(1/2) = 1.77$ where Γ is the Euler function, C_A is the concentration of acceptor ions and R_{DA} is the critical transfer distance defined as the separation at which the probability of energy transfer between a donor–acceptor pair equals to inherent probability of donor decay.

Figure 5 compares decay curves of the 3H_4 luminescence recorded for $YVO_4:0.5 \text{ at. \% Tm}^{3+}$ and for $YVO_4:1 \text{ at. \% Tm}^{3+}, 5 \text{ at. \% Eu}^{3+}$. The measured decay curve of the 3H_4 level of Tm^{3+} in the former crystal is exponential with estimated lifetime of 176 μs . The radiative lifetime calculated according to the Judd–Ofelt theory is equal to 224 μs [16]. In fluoride matrices at low thulium concentration the quantum efficiency of the 3H_4 level of Tm^{3+} is close to unity. However, oxide materials are characterized by higher phonon frequencies (around 900 cm^{-1} in YVO_4 [17]) than in fluoride crystals. Consequently, the 3H_4 quantum efficiency is reduced owing to considerably higher nonradiative relaxation probability from 3H_4 emitting level down to the 3H_5 level [6]. Experimental decay curve recorded with co-doped crystal fits well the time dependence predicted by the Inokuti–Hirayama expression (5–6) with parameter $\alpha = 3.37$. Evaluated values of $R_{DA} = 15.4 \text{ \AA}$ and $C_{DA} = 7.58 \times 10^{-38} \text{ cm}^6 \text{ s}^{-1}$ are considerably higher than those values reported for $LiYF_4:Tm, Eu$ [5] corresponding $R_{DA} = 8.89 \text{ \AA}$ and $C_{DA} = 2, 47 \times 10^{-40} \text{ cm}^6 \text{ s}^{-1}$. The measured decay curve of the 3H_4 level of Tm^{3+} in $YVO_4:1 \text{ at. \% Tm}^{3+}$,

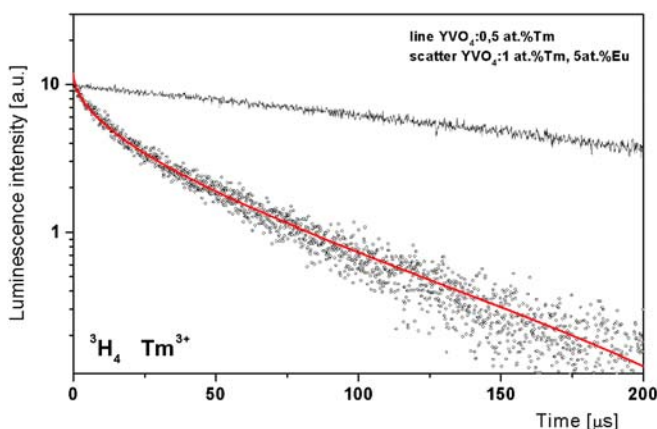


FIGURE 5 Luminescence decays of the thulium 3H_4 level in $YVO_4:0.5 \text{ at. \% Tm}$ and in the $YVO_4:1 \text{ at. \% Tm}:5 \text{ at. \% Eu}$ crystals measured at 300 K. The solid line presents the fitted curve (Inokuti–Hirayama model)

5 at. $\% \text{Eu}^{3+}$ crystal is non-exponential and therefore a mean lifetime τ_m defined as:

$$\tau_m = \frac{\int I(t) dt}{I_0} \quad (7)$$

where I_0 is the initial intensity seems to be more convenient to characterize the decay. Thus, mean lifetime of the 3H_4 level of Tm^{3+} in the presence of Eu^{3+} ions is evaluated to be $\tau_m = 37 \mu\text{s}$.

With this result and the 3H_4 radiative lifetime $\tau_0 = 224 \mu\text{s}$ [15], the quantum efficiency defined as $\eta_f = \tau_m/\tau_0$ for the 3H_4 level of Tm^{3+} in 1 at. $\% \text{Tm}^{3+}$, 5 at. $\% \text{Eu}^{3+}:YVO_4$ is found to be 0.16, a value slightly higher than 0.15 reported for 1 at. $\% \text{Tm}^{3+}$, 3 at. $\% \text{Eu}^{3+}:LiYF_4$ [5]. The energy transfer rate from Tm^{3+} to Eu^{3+} ions W_{Tm-Eu} , can be calculated from the Tm^{3+} decay times obtained for samples with and without Eu^{3+} ions:

$$W_{Tm-Eu} = \frac{1}{\tau_{Tm,Eu}} - \frac{1}{\tau_{Tm}} \quad (8)$$

where τ_{Tm} and $\tau_{Tm,Eu}$ are the emission decay times of the Tm^{3+} - states without and with the presence of Eu^{3+} ions in the YVO_4 crystals, respectively. With the lifetime values mentioned above the energy-transfer rates from Tm^{3+} to Eu^{3+} for $YVO_4:1 \text{ at. \% Tm}^{3+}, 5 \text{ at. \% Eu}^{3+}$ are $\sim 17027 \text{ s}^{-1}$ for 3H_4 and 14400 s^{-1} for 3F_4 levels of thulium.

Emission cross-section spectra associated with the 3H_4 – 3F_4 transition of Tm^{3+} for σ and π polarization in 1 at. $\% \text{Tm}^{3+}$, 5 at. $\% \text{Eu}^{3+}:YVO_4$ are shown in Fig. 6. The spectra were excited by a cw radiation at 641.7 nm emitted by krypton ion laser and calculated using the so-called Fuchtbauer–Ladensburg method [18]. It can be seen that most remarkable feature presented by the stimulated emission spectra is presence of two intense lines centered at 1466 and 1480 nm for both σ and π polarization. Four-level laser channel associated with the 3H_4 – 3F_4 transition is advantageous because

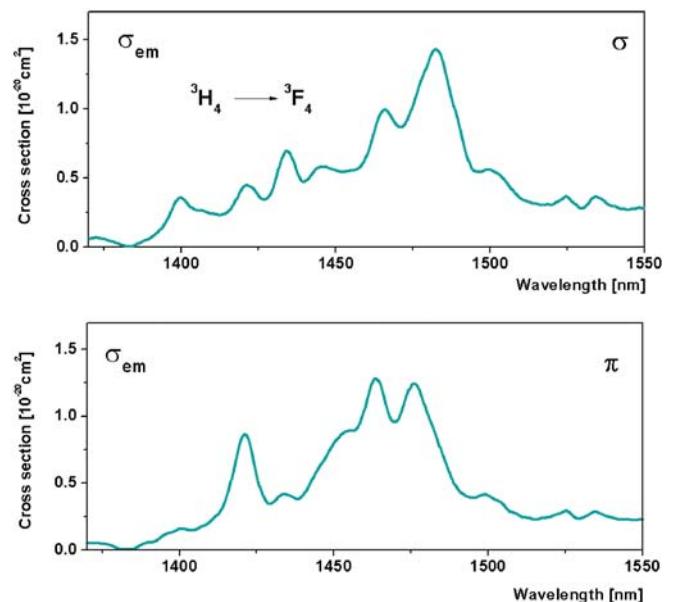


FIGURE 6 π and σ emission cross-section spectrum of Tm^{3+} in 1 at. $\% \text{Tm}^{3+}$, 5 at. $\% \text{Eu}^{3+}:YVO_4$ at around 1.5 μm

in contrast to the laser operation associated with the ${}^3F_4-{}^3H_6$ transition the terminal level is not the ground multiplet whose crystal field splitting of 360 cm^{-1} in YVO_4 is relatively small [11]. The maximum value of σ_{em} for σ polarization at around 1500 nm is considerably higher than that calculated for thulium-doped LiYF_4 crystal [5].

4 Conclusions

The energy transfer processes and relaxation dynamics of excited states were analysed for $\text{Tm}^{3+}-\text{Eu}^{3+}$ system in YVO_4 crystal. The europium ions shorten effectively the 3F_4 lifetime and simultaneously enhance nonradiative relaxation of the 3H_4 level of Tm^{3+} . Inokuti–Hirayama classical energy transfer model was applied successfully to describe the time dependence of luminescence decay from the potential upper laser level 3H_4 of Tm^{3+} . The quantum efficiency of the 3H_4 level of Tm^{3+} in YVO_4 is sufficiently high to justify the consideration of laser operation associated with ${}^3H_4-{}^3F_4$ transition. The distribution of emission band intensity and relatively high value of emission cross section at near 1480 nm are favorable for infrared laser emission in the $\text{YVO}_4:\text{Tm}, \text{Eu}$ system. Intensity of a broad pump band associated with the ${}^3H_6-{}^3H_4$ transition of Tm^{3+} at around 800 nm is also advantageous for laser operation. Evaluated C_{DA} microparameters characterizing the processes of ion–ion interaction may be useful in assessment of optimal concentrations of Tm^{3+} and Eu^{3+} ions in the investigated material.

ACKNOWLEDGEMENTS This work was supported by Polish Ministry of Science and Information Society Technologies within a grant for years 2005–2006.

REFERENCES

- 1 I.R. O'Connor, *Appl. Phys. Lett.* **9**, 407 (1966)
- 2 K. Ohta, H. Saito, M. Obara, N. Djeu, *Jpn. J. Appl. Phys.* **32**, 1651 (1993)
- 3 A.A Kaminskii, *Phys. Stat. Solidi A* **200**, 215 (2003)
- 4 R.C. Stoneman, L. Esterowitz, *Opt. Lett.* **6**, 232 (1991)
- 5 A. Braud, S. Girard, J.L. Doualan, R. Moncorge, *IEEE J. Quantum Electron.* **QE-34**, 2246 (1998)
- 6 J.T. Vega-Durán, L.A. Diáz-Torres, M.A. Meneses-Nava, J.L. Maldonado-Rivera, O. Barbosa-García, *J. Phys. D Appl. Phys.* **34**, 3203 (2001)
- 7 B.M. Antipenko, R.V. Dumbbravyanu, Y.E. Perlin, O.B. Rabu, L.K. Sukhareva, *Opt. Spectrosc.* **59**, 377 (1985)
- 8 W. Ryba-Romanowski, M. Berkowski, B. Viana, P. Aschehoug, *Appl. Phys. B* **64**, 525 (1997)
- 9 R.M. Percival, D. Szebesta, S.T. Davey, *Electron. Lett.* **28**, 1866 (1992)
- 10 F.S. Ermeneux, C. Goutaudier, R. Moncorge, M.T. Cohen-Adad, M. Bettinelli, E. Cavalli, *Opt. Mater.* **8**, 83 (1997)
- 11 R. Lisiecki, W. Ryba-Romanowski, T. Łukaszewicz, H. Mond, K. Petermann, *Laser Phys.* **15**, 306 (2005)
- 12 K.D. Knoll, *Phys. Stat. Solidi B* **45**, 553 (1971)
- 13 F. Auzel, *Phys. Rev. B* **13**, 2809 (1976)
- 14 M. Yokota, J. Tanimoto, *J. Phys. Soc. Jpn.* **22**, 779 (1967)
- 15 M. Inokuti, F. Hirayama, *J. Chem. Phys.* **43**, 1978 (1965)
- 16 C. Xueyuan, L. Zundu, *J. Phys.: Condens. Matter* **9**, 7981 (1997)
- 17 E.D. Reed, H.W. Moos, *Phys. Rev. B* **8**, 980 (1973)
- 18 Y. Gujot, H. Manaa, J.Y. Rivoire, R. Moncorge, N. Garnier, E. Descoix, M. Bon, P. Laporte, *Phys. Rev. B* **51**, 784 (1995)